UC Irvine
UC Irvine Previously Published Works

Title
Measurement of Heat Flux and Heat Transfer Coefficient During Continuous Cryogen Spray Cooling for Laser Dermatologic Surgery

Permalink
https://escholarship.org/uc/item/5382r6kg

Journal
IEEE Journal of Selected Topics in Quantum Electronics, 7(6)

ISSN
1077-260X

Authors
Aguilar, Guillermo
Verkruysse, Wim
Majaron, Boris
et al.

Publication Date
2001

DOI
10.1109/2944.983307

Copyright Information

Peer reviewed

Measurement of Heat Flux and Heat Transfer Coefficient During Continuous Cryogen Spray Cooling for Laser Dermatologic Surgery

Guillermo Aguilar, Wim Verkruysse, Boris Majaron, Lars O. Svaasand, Enrique J. Lavernia, and J. Stuart Nelson

Abstract—**Cryogen spray cooling (CSC) has been used for selective epidermal cooling of human skin during laser therapy of patients with port wine stain (PWS) birthmarks. Unfortunately, current commercial CSC devices do not provide optimal cooling selectivity and, therefore, provide insufficient epidermal protection for some PWS patients. To assist in the development of improved atomizing nozzle designs, a reliable method to quantify the CSC heat flux is needed. We introduce a novel method to determine the heat flux (q_s) and heat transfer coefficient (h) at the surface of a sprayed object, based on measurements of steady-state temperature gradients along a thin copper rod during continuous cryogen spraying. For an atomizing nozzle of inner diameter $d_N = 0.7$ mm, we found that q_s varies from 15 to 130 W/cm^2 and h increases nonlinearly from 15 000 to 35 000 W/m^2·K in the explored range of surface temperatures (T_s, from -32 to -7°C). Values of q_s obtained with a wider diameter nozzle ($d_N = 1.4$ mm) are approximately twice as large than those of the narrow nozzle. The corresponding values of h are significantly higher (32 000–40 000 W/m^2·K) and almost independent of T_s within the same temperature range. When combined with fast flashlamp photography (FFLP) of spray shapes and sprayed surfaces, the results demonstrate that the liquid cryogen layer, as deposited by finely atomized sprays from narrower nozzles, can significantly impair q_s. In contrast, the higher-momentum impact of coarser sprays from wider nozzles reduces the thickness of the liquid layer in the impact area and/or enhances convection within it, yielding a larger q_s.**

Index Terms—**Cryogen spurt, nozzles, port wine stain, skin cooling.**

G. Aguilar is with the Center for Biomedical Engineering and the Beckman Laser Institute and Medical Clinic, University of California, Irvine, CA 92162 USA (e-mail: gaguilar@bli.uci.edu).

W. Verkruysse is with the Beckman Laser Institute and Medical Clinic, University of California, Irvine, CA 92162 USA.

B. Majaron is with the Jožef Stefan Institute, Jamova 39, SI-1000 Ljubljana, Slovenia, and also with the Beckman Laser Institute and Medical Clinic, University of California, Irvine, CA 92162 USA.

L. O. Svaasand is with the Beckman Laser Institute and Medical Clinic, University of California, Irvine, CA 92162 USA and also with the Department of Physics and Electronics, Norwegian University of Science and Technology, Trondheim, Norway.

E. J. Lavernia is with the Center for Biomedical Engineering, University of California, Irvine, CA 92162 USA and also with the Department of Chemical Engineering and Materials Science, University of California, Irvine, CA 92162 USA.

J. S. Nelson is with the Center for Biomedical Engineering and also with the Beckman Laser Institute and Medical Clinic, University of California, Irvine, CA 92162 USA.

Publisher Item Identifier S 1077-260X(01)11186-X.

I. INTRODUCTION

DURING laser treatment of skin lesions, such as port wine stain (PWS) birthmarks, two competing absorbers of light can be identified: melanin, mostly located within the epidermis, and hemoglobin, located in the targeted blood vessels. Unfortunately, the absorption of energy by melanin not only reduces the amount of energy that can be delivered to and absorbed by the PWS blood vessels, but it also causes heating of the epidermis, which, if not controlled, may lead to blistering, scarring, or dyspigmentation [1]. The latter poses an upper limit on the maximum permissible laser radiant exposure—a major limitation for the treatment of patients with darker skin types. Applying a cryogen spurt to the skin for an appropriately short period of time (10–100 ms), allows selective epidermal cooling prior to laser exposure, while the temperature of the deeper targeted structures, PWS vessels, remains relatively unaffected [2]–[4]. Such cooling allows high-energy laser pulses to cause thermal damage to the PWS while protecting the epidermis. Inevitably, however, thermal diffusion induces some cooling of the PWS vessels, depending on spurt duration, spray temperature and quality of the thermal contact between the cryogen and skin. Introduction of cryogen spray cooling (CSC) technology has enabled safe use of high-energy laser pulses, improving therapeutic outcome of PWS [1], [3], [5], telangiectasias, hemangiomas [6], rhytides [7], and laser hair removal [8]. (A recent overview of mechanisms, technology and clinical experience with CSC can be found in Nelson *et al.* [9].)

Despite its relatively wide use, the exact mechanisms involved in CSC remain incompletely understood. Consequently, current delivery systems may not provide optimal cooling selectivity and efficiency. Recent studies aimed at improving our understanding and optimizing the design and application of the CSC technology can be divided into two groups. The first group of studies focuses on the characteristics of liquid cryogen atomization and dynamics of evaporation as the droplets travel from the nozzle to the skin surface. It has been reported that the average droplet diameter (D) and spray temperature (T) of sprays produced by straight-tube nozzles with inner diameter $d_N = 0.5$–0.7 mm are noticeably different from those with nozzles having $d_N = 1.4$ mm [10]. Aguilar *et al.* [11], [12] proposed a single-droplet evaporation model to predict the variations of average D and T with distance from the nozzle (x). The model predictions matched $T(x)$ for various straight-tube nozzles within an error margin of ± 2°C [10].

The second group of studies focuses on the mechanisms of cryogen-surface interaction and measurements of the heat transfer coefficients (h) at the cryogen-surface interface. Torres *et al.* [13] used a block of epoxy with micro-thermocouples embedded at various depths, including one on the surface. From thermocouple measurements during a 100-ms cryogen spurt, they have determined a cryogen temperature of $T_c = -44\,°C$ and an average $h = 2400\ \mathrm{W/m^2 \cdot K}$. A recent attempt to use the same experimental approach in our group with a straight-tube nozzle ($d_N = 1.4$ mm) resulted in a markedly higher h value of $\sim 10\,000\mathrm{W/m^2K}$ at $T_c = -49\,°C$ [14]. However, a stability analysis suggested a very large uncertainty interval for that value of $h(+20\,000/-4000\ \mathrm{W/m^2 \cdot K})$ and $\pm 1\,°C$ for T_c [14]. The large uncertainty in h is a manifestation of the instability, related to the well-known inherent ill-posedness of inverse heat diffusion problems. The marked skewedness of the uncertainty interval points to a strong nonlinear relationship between the heat flux (q_s) and the thermocouple response time [15]. For large values of h, the thermal resistance of the cryogen layer becomes too low compared to that of epoxy and, consequently, the epoxy's thermal diffusivity becomes the physical limitation for the amount of heat that can be extracted per unit time, causing the method to become insensitive to variations in h.

Besides this inherent limitation of the epoxy-block method, there are other effects that contribute to the inaccuracy of measurements, or introduce unknown systematic errors to the measured data [14], [16]. Such effects include inaccurate positioning and large size of the thermocouple beads relative to their distance from the cooled surface—a large source of systematic errors considering the steep temperature gradients involved; inaccurate estimation of the response time of the thermocouple beads; inaccurate determination of epoxy's thermal properties, which we found to be strongly temperature dependent; heat flux along the thermocouple wires, which may severely affect the measurement and/or perturb the temperature field evolution in the epoxy; and a long cryogen spray development time (20–30 ms) [10], during which the heat flux is not constant [17].

In view of this, while the epoxy-block method may be a useful instrument to study the temperature field evolution in human skin, the related quantitative determination of h lacks the accuracy and reproducibility required to monitor changes in cooling dynamics induced by variations in nozzle geometry or other spraying conditions.

To this end, we have developed an alternative measurement method, which enables reproducible and much more accurate determination of q_s and h during continuous CSC. The main difference from the previously discussed method is that temperature is measured in a metal substrate, rather than epoxy. The significantly higher metal thermal conductivity and diffusivity ensure much lower temperature gradients and faster establishment of steady-state conditions when these gradients can be reliably determined. In addition, the thermal properties of pure metals are known with high accuracy and vary only marginally within the temperature interval being studied. Furthermore, shaping the detecting element as a thin rod ensures the validity of a one-dimensional (1-D) approximation, which is used in the forthcoming analysis. It should be noted that this feature also enables characterization of laterally inhomogeneous

TABLE I
LENGTHS (l_N) AND INNER DIAMETERS (d_N) OF THE FOUR STRAIGHT-TUBE NOZZLES

Nozzle	l_N (mm)	d_N (mm)
Short narrow (SN)	32	0.7
Short wide (SW)	32	1.4
Long narrow (LN)	64	0.7
Long wide (LW)	64	1.4

sprays—unlike the epoxy-block method. This is a very important aspect because temperature variations higher than $10\,°C$ have been measured over lateral distances less than 3 mm (90 μm below the surface of a cooled epoxy block) [14]. Finally, the proposed measurements can be performed at different fixed target surface temperatures (T_s), which provide new insight into the mechanisms of heat transfer across the surface-cryogen interface during CSC.

The basic elements of the metal-rod method and preliminary data have been presented earlier [14]. In this work, this method is utilized to investigate systematically CSC with straight-tube atomizing nozzles of different dimensions. The results fully comply with an earlier presented hypothesis [14] stating that a thin layer of liquid cryogen, which is often formed on the sprayed surface during CSC [18], [19], may present a barrier to heat extraction from skin due to its relatively low thermal conductivity. Our results also demonstrate directly that coarser sprays, as produced by straight-tube nozzles having $d_N = 1.4$ mm can provide up to two times higher cooling rates as compared to finely atomized sprays of nozzles having $d_N = 0.5–0.7$ mm. This further emphasizes the importance of spray droplet momentum in CSC, which is in good agreement with the hypothesis put forward by Verkruysse *et al.* [14], as well as with recent systematic measurements of cryogen spray properties and h as a function of distance from the atomizing nozzle [18].

II. METHODS

A. Cryogen Delivery and Nozzles

The cryogen utilized in the present study is the same as that used in previous studies and current clinical devices (1,1,1,2 tetrafluoroethane, also known as R134a, with boiling temperature $T_b \approx -26\,°C$ at atmospheric pressure.) Cryogen is kept in a container at saturation pressure (approximately 6.6 bar at $25\,°C$) and delivered through a standard high-pressure hose to an electronically controlled fuel injector, to which various atomizing nozzles were attached.

Four straight-tube nozzles made of stainless steel of two different lengths (l_N) and two different inner diameters (d_N) were constructed. The tubes were soldered to custom-made copper couplings, which in turn fitted tightly around the fuel injector. Table I shows the dimensions and acronyms of the four nozzles used in this study. The dimensions of the SN nozzle were based on the geometry of a commercial cryogen spray device

(DCD for ScleroPlus, by Candela, Wayland, MA; $l_N \approx 25$ mm, $d_N \approx 0.75$ mm); the others were scaled by a factor of two with respect to the SN.

B. Fast Flashlamp Photography (FFLP)

A progressive-scan CCD camera with a shutter speed of 60 μs (9700 TMC by Pulnix, Sunnyvale, CA) was used to acquire images of the spray shapes and of the cryogen layer deposited on a black plastic plate 30 ms after application of 20 ms spurts. A fast flashlamp (FX-1160, EG&G Electronics, Salem, MA) provided illumination gating by 5-μs-long pulses that "freeze" the images of flying cryogen droplets. The supporting electronics enabled acquisition of image sequences at 30 frames/s with precisely controlled delays relative to onset of the cryogen spurt.

The spray shape images were taken under identical conditions, with the camera axis perpendicular to the spray axis. The field of view from a distance of 130 mm was approximately 17×14 mm. The flashlamp was positioned in the same horizontal plane and directed toward the nozzle tip at an angle of 30° with respect to the camera axis. For images of the cryogen-sprayed target, the camera was aimed perpendicular to the target surface at a distance of 130 mm. The spray was aimed toward the block at an angle of $\sim 20°$ with respect to the camera axis. The flashlamp was placed on the opposite side of the camera, aimed at the sprayed surface at a 45° angle with respect to the normal at a distance of 80 mm.

C. Cryogen Spray Temperature

Cryogen spray temperature was measured by inserting a type-K thermocouple with a bead diameter of 300 μm (5SC-TT-E-36 by Omega, Stamford, CT) into the center of the spray cone at approximately 50 mm from the nozzle tip. Also, an array consisting of eight identical thermocouples was built to determine lateral variations of spray temperature. Beads were mounted into small indentations along the edge of a thin plastic foil (≈ 150 μm thick) at uniform distances of approximately 3 mm and the foil was supported by a rigid frame. Thermocouple readings were acquired and converted to temperature data using an A/D converter board and dedicated software (instruNet, Omega Engineering, Stamford, CT).

D. Heat Flux (q_s) and Heat Transfer Coefficient (h)

The experimental apparatus consisted of a copper rod (alloy 110), with a diameter, $d_{\rm rod} = 6.35$ mm (1/4-in) and length, $z_{\rm rod} = 100$ mm. The end of the rod was sprayed with cryogen and surrounded by a 12-mm-thick epoxy platform, which provided a flat target surface to prevent dripping of liquid cryogen onto the copper rod (Fig. 1). Concurrently, a constant but adjustable heat source was applied to the opposite end of the rod. The heat source consisted of either a constant flux of hot air from a hair dryer (low heat fluxes), or a pair of soldering irons (higher heat fluxes) brought into thermal contact with the copper rod at varying distances from the sprayed end. Four type-K thermocouples with a bead diameter of ~ 300 μm were attached to the side of the copper rod at known distances varying from $z = 20$–9 mm from the sprayed surface (Fig. 1). The rod was
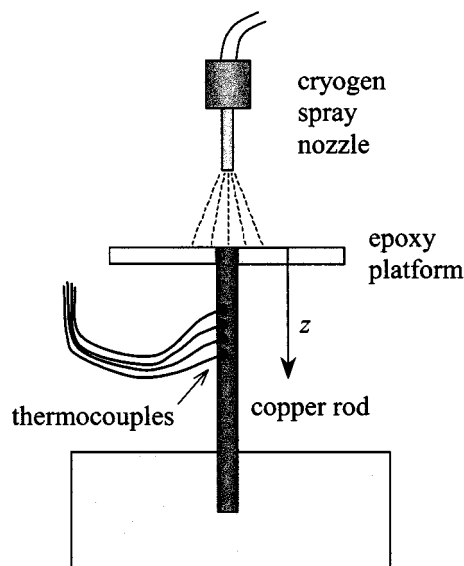

Fig. 1. Schematic of the metal-rod experimental setup. The distal end of the rod is in contact with an adjustable continuous heat source.

wrapped into insulation material to reduce lateral loss of supplied heat.

This method requires the temperature profile inside the rod to reach steady-state conditions. The time for this to happen may be estimated by the heat diffusion time for the whole rod: $\tau = z_{\rm rod}^2/\alpha_{Cu} \approx 90s$, where α_{Cu} is the copper thermal diffusivity ($\alpha_{Cu} = 1.12 \times 10^{-4}$ m^2/s). Therefore, to ensure steady-state conditions, all temperature measurements were taken at least 270 s after onset of spraying or any change in the supplied heat power.

Only one equation was required for the analysis, the convective (also called radiative, or Robin) boundary condition [20] at the sprayed end of the copper rod is

$$\kappa_{Cu} \left(\frac{dT}{dz} \right)_{z=0^+} = h\left(T_s - T_c\right). \tag{1}$$

Here, κ_{Cu} is the thermal conductivity of copper ($\kappa_{Cu} = 397$ W/m·K), $T_s = T(z = 0^+)$ is the rod surface temperature and T_c is the average temperature of the cryogen layer on the sprayed surface. This relationship equates the heat flux conducted through the copper rod with the rate of convective and evaporative heat extraction by the cryogen spray, expressed by h.

In these experiments, the temperature gradient at the surface, $(dT/dz)_{z=0^+}$ and surface temperature of the copper rod, T_s, were determined by extrapolation of best fit through thermocouple measurements acquired simultaneously along the length of the rod. Evidently, heat flux across the end surface of the copper rod (q_s) is then easily calculated as $q_s = \kappa_{Cu} (dT/dz)_{z=0^+}$.

A series of measurements was performed while varying q_s which can be achieved by adjusting the heat source power, or by changing the effective length of the copper rod (i.e., distance between the heat source and the sprayed end). To provide additional insight into the involved heat transfer mechanisms, the
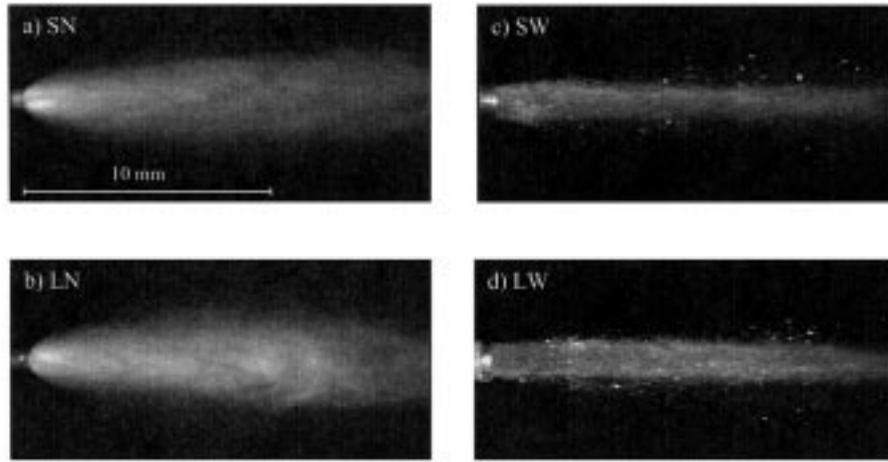
Fig. 2. FFLP images of cryogenic sprays from four straight-tube nozzles (see Table I for nozzle dimensions). The field of view is approximately 17 mm.
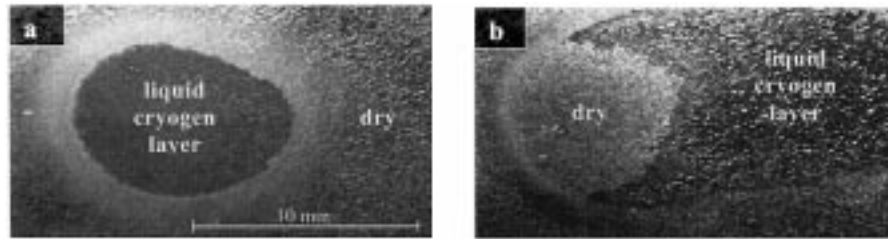

Fig. 3. Images of a sprayed black surface, taken 30 ms after the end of a 20 ms spurt from the (a) LN and (b) LW nozzles. Cryogen was sprayed from the left side at an angle of about 20° with respect to the normal to the surface. The area sprayed with the LN nozzle (a) is covered by a liquid cryogen layer, whereas with the LW nozzle (b) the target area is dry.

determined q_s were then plotted as a function of corresponding T_s. According to (1), if the values of h and T_c were constant within the range of the surface temperatures involved, the experimental points of the q_s versus T_s graph should lie on a straight line with a slope equal to h, intersecting the temperature axis at T_c.

III. RESULTS

A. Fast Flashlamp Photography (FFLP)

Fig. 2 shows images of spray shapes produced by the four nozzles. For the two *narrow* nozzles (SN and LN) a cone-shaped and finely atomized spray is evident [Fig. 2(a) and (b)], while for the *wide* nozzles (SW and LW) the cryogen exits in a jet-like fashion [Fig. 2(c) and (d)], resulting in coarser atomization. It appears that the influence of nozzle length on spray characteristics is minimal when compared to the marked influence of nozzle diameter. For this reason, subsequent measurements comparing spray features were carried out using either the pair of *short* (SN versus SW) or *long* (LN versus LW) atomizing nozzles.

Fig. 3(a) and (b) shows images of liquid cryogen deposition on the flat surface of a black plastic block, with the LN and LW nozzles, respectively. Each photograph is taken 30 ms after the end of a 20 ms spurt. Fig. 3(a) shows an oval-shaped liquid cryogen layer, surrounded by a ring of snow/frost and then a dry area outside this ring. In contrast, the center of the sprayed area in Fig. 3(b) is dry, while an extensive cryogen liquid layer persists adjacent to the impact site.

A comparison between Figs. 2 and 3 suggests that fine-droplet sprays produced by the *narrow* nozzles are deposited more gently in the central zone of the sprayed surface and, therefore, allow the build up of a liquid layer when the delivered mass flux exceeds the rate of evaporation. In contrast, the *wide* nozzles produce coarser sprays, capable of pushing excess cryogen aside from the impact area, thus causing the latter to dry quicker after spurt termination.

B. Spray Temperature Measurements

Fig. 4 presents the lateral variation of spray temperature (i.e., average spray droplet temperature), as measured with the linear array of eight thermocouples. The array was positioned 50 mm from the nozzle tip. A commercial atomizing nozzle (DCD for ScleroPlus) with d_N slightly larger (≈ 0.75 mm) than our *narrow* nozzles was used for these measurements. The bars in Fig. 4 represent the standard deviation computed from five consecutive measurements. All measurements were performed after both the spray and thermocouples reached thermal steady-state conditions (i.e., more than 120 ms after beginning of the spurt). The results indicate that spray temperature is practically constant ($\sim -58\,°C$; dashed line) up to 6 mm away from the spray axis, which is twice the radius of the copper rod detector.

C. Heat Flux (q_s)

Fig. 5(a) and (b) shows steady-state temperatures measured along the copper rod, $T(z)$, as a function of distance from the
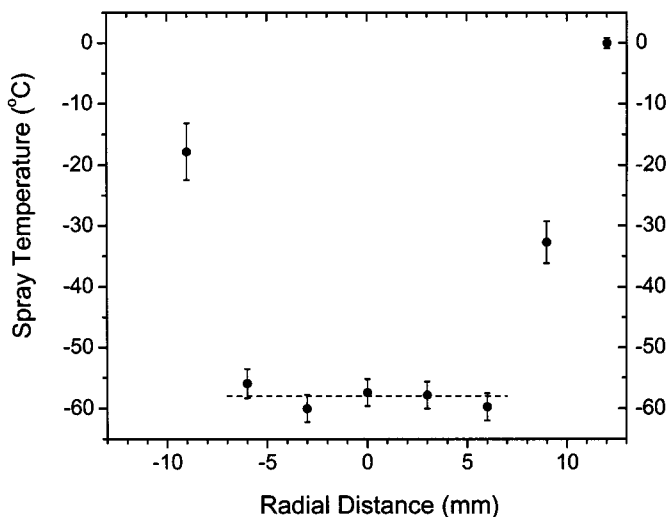
Fig. 4. Lateral variation of spray temperature. Measurements were taken with an array of eight type-K thermocouples, each with a bead diameter of 300 μm, positioned 50 mm from the nozzle tip. Note the small spray temperature variation up to 6 mm from the spray axis.
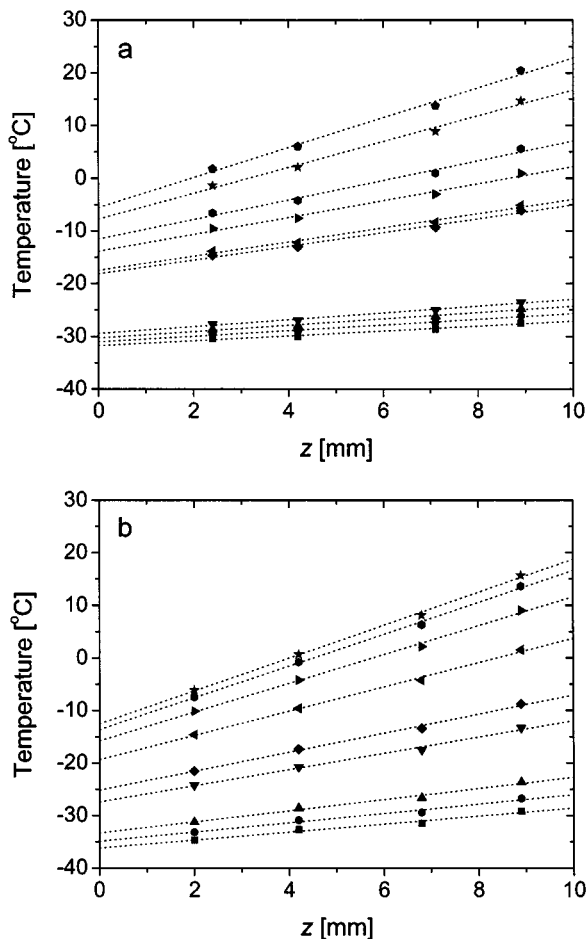

Fig. 5. Steady-state temperature measurements as a function of distance from the sprayed surface of the rod (z). (a) and (b) correspond to measurements carried out with the SN and SW nozzles, respectively. Each line represents a linear fit through four simultaneous thermocouple readings obtained for different powers of the heat source.
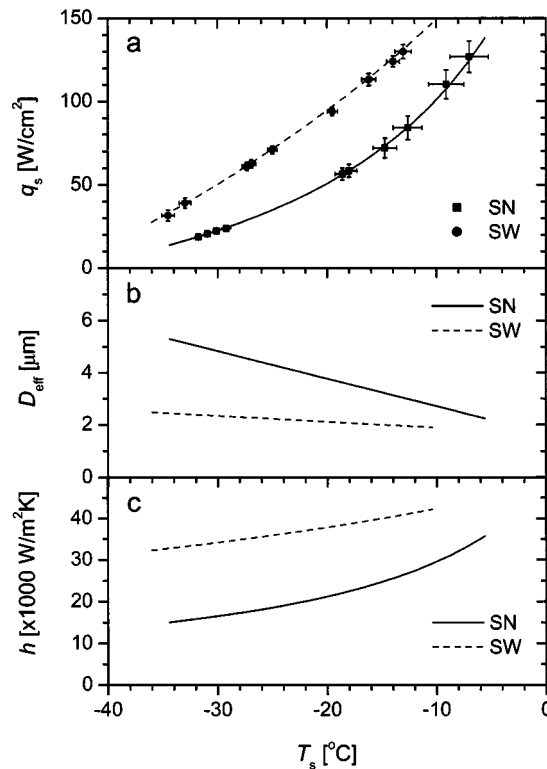

Fig. 6. (a) Heat flux through the copper rod surface, q_s, as a function of surface temperature, T_s, as obtained from linear fits to data in Fig. 5(a) and 5(b). (b) Effective cryogen layer thickness (D_{eff}) computed from (2) as a function of T_s for the SN (solid line) and SW (dashed line) nozzles, respectively. This computation assumes that q_s in (a) can be accounted for by conduction through a liquid cryogen layer of thickness D_{eff}, which depends linearly on T_s. (c) Heat transfer coefficients (h), as computed from (3) for the SN (solid line) and SW (dashed line) nozzles, respectively.

through the four simultaneous thermocouple readings, obtained using different heat source powers. In the presented examples, we determined that an attempt to use parabolic fits did not improve the overall accuracy of the procedure. As evident from (1), higher surface temperatures correspond to larger temperature gradients, which, in turn, reflect higher heat fluxes through the rod.

Values for q_s obtained by multiplying the above-determined temperature gradients (ranging from 0.4 to 3.2 K/mm) with κ_{Cu}, are presented in Fig. 6(a) as a function of corresponding surface temperatures, T_s (from $-34\,^\circ$C to $-7\,^\circ$C). The results obtained with the SN and SW nozzles are represented by squares and circles, respectively. The bars indicate the standard errors of q_s and T_s from the linear fitting to thermocouple readings. Fig. 6(a) demonstrates that for the range of T_s studied, q_s obtained with the SW nozzle is approximately twice as large than with the SN nozzle. With the SN nozzle, q_s values range from ~ 15 W/cm^2 at $T_s = -32\,^\circ$C (6 $^\circ$C below T_b), up to ~ 130 W/cm^2 at $T_s = -7\,^\circ$C (almost 20 $^\circ$C above T_b).

The $q_s(T_s)$ dependence for the SW nozzle is almost linear, indicating a rather constant value of h over the range of T_s ($-34\,^\circ$C to $-13\,^\circ$C). In contrast, with the SN nozzle, the same relationship is evidently nonlinear, indicating that h is increasing significantly with increasing T_s. We can tentatively attribute these observations to the following effects: in our experimental design, higher surface temperatures are intrinsically

sprayed surface, z, for experiments using the SN and SW nozzles, respectively. Each line in these graphs represents a linear fit

related to higher heat fluxes, which should reduce the thickness of the liquid cryogen layer due to enhanced evaporation. Consequently, the thermal barrier presented by the liquid layer is reduced, leading to increased heat *conduction* across the layer. In addition, a higher surface temperature and heat flux should enhance boiling, thereby increasing the *convective* contribution to heat transport across the liquid layer.

D. Heat Transfer Coefficient (h)

Since the relationship $q_s(T_s)$ presented in Fig. 6(a) deviates from linear dependence, the value of h can not be computed directly from (1). Therefore, we introduce an oversimplified model, where the measured q_s is ascribed exclusively to heat conduction through a layer of liquid cryogen with thickness D_{eff}

$$q_s = \kappa_{\text{cryo}} \frac{(T_s - T_c)}{D_{\text{eff}}}. \tag{2}$$

Here, κ_{cryo} is the thermal conductivity of the liquid cryogen ($\kappa_{\text{cryo}} = 0.0824$ W/mk). As a first approximation, let us assume further that D_{eff} depends on T_s in a linear manner. When this relationship is inserted into (2), the resulting function $q_s(T_s)$ can be fitted to experimental data in Fig. 6(a). The two best-fit curves presented therein show that a good match could be obtained for both data sets.

The corresponding linear dependencies $D_{\text{eff}}(T_s)$ are presented in Fig. 6(b). For the SW nozzle, D_{eff} is almost constant over the studied range (dashed line), whereas for the SN, it is larger and strongly decreasing with T_s (solid line)—in perfect agreement with the discussion in Section III-C. Quantitatively, all obtained values of D_{eff} are significantly lower then the expected cryogen layer thickness ($\sim 20 \ \mu$m) [21], which demonstrates that convective, rather than conductive, contribution to heat transfer across the layer is dominant for both nozzles studied.

From (1) and (2), h can now be calculated as

$$h(T_s) = \frac{\kappa_{\text{cryo}}}{D_{\text{eff}}(T_s)}. \tag{3}$$

The results in Fig. 6(c) indicate that h values are increasing with T_s over the range of 15 000–35 000 W/m$^2 \cdot$K for the SN and 32 000–42 000 W/m$^2 \cdot$ K for the SW nozzle. Therefore, h with the SW nozzle is, thus, approximately twice as large as that for the SN and much less dependent on the surface temperature. It is important to note that despite the fact that our linear model of the $D_{\text{eff}}(T_s)$ dependence is not supported by theory, the obtained values for h are meaningful, as long as the corresponding curves $q_s(T_s)$ match the experimental data well.

IV. DISCUSSION

In Fig. 2(a) and 2(b), it is noted that *narrow* nozzles produce cone-shaped finely atomized sprays, while *wide* nozzles produce jet-like coarser sprays [Fig. 2(c) and 2(d)]. It appears that within the investigated range, nozzle diameter (d_N) is more critical than length (l_N) in determining spray shape.

Indeed, our recent work [10] has demonstrated that sprays with similar morphology (i.e., sprays produced by nozzles of same d_N) produce similar droplet sizes and spray temperatures

as a function of distance from the nozzle tip, regardless of l_N. For example, at a distance of 50 mm, the Sauter mean diameter of spray droplets was 4–5 μm for the *narrow* straight-tube nozzles used in the present study and 10–15 μm for the *wide* nozzles. Qualitatively, the same observation was recently reported by Pikkula *et al.* [22]. Our measurements also indicated a significant influence of l_N on the average droplet velocity [10]. As discussed below, average droplet velocity may have an impact on cryogen deposition and spreading on the target surface and, thus, influence cooling efficiency.

Spray morphology and characteristics can be further associated with spray-surface interactions. Images presented in Fig. 3 indicate that fine sprays (*narrow* nozzles) form a cryogen pool [dark elliptical area in the center of Fig. 3(a)], which is noted in the region of spray impingement 30 ms after spurt termination. In fact, our recent investigations showed that such a layer could persist even longer on warm *in vivo* human skin; a persistence time of 500 ms was documented after an 80-ms spurt from a commercial, 0.5-mm-diameter nozzle (DCD for Gentle-Lase) [19]. In contrast, for coarse sprays (*wide* nozzles), there is no sign of a cryogen pool 30 ms after spurt termination on the site of spray impingement [the relatively bright, circular spot on the left side of Fig. 3(b)], although a larger cryogen pool is seen adjacent to it. The total cooled area (i.e., the zone of spray impingement plus the adjacent cryogen pool), is considerably larger for coarse as opposed to fine sprays [18], corresponding well to the higher mass flux of liquid cryogen through the wider atomizing orifice.

Based on results presented herein (Figs. 2 and 3) and more detailed cryogen spray characterization reported elsewhere [10], [18], we can conclude that cryogen droplets from fine sprays have lower momentum (i.e., droplets are smaller and slower). As the spurt develops, these droplets are gently deposited on the surface, forming a layer that increases in thickness since the mass flow rate exceeds the evaporation rate of the cryogen layer [17]. Furthermore, droplets with low momentum cannot break through this cryogen layer, therefore coalescing with its surface and forming an even thicker layer. Due to the relatively low thermal conductivity of liquid cryogen, the presence of this layer is detrimental to the heat flux from the skin surface (Fig. 6). In contrast, larger momentum droplets from coarse sprays (*wide nozzles*) cause some cryogen droplets to bounce off the sprayed object, resulting in a thinner layer at the center of the sprayed surface. Moreover, such large momentum droplets can pierce through the cryogen layer and displace some of the warmer liquid cryogen toward the periphery. Consequently, both increased heat conduction across the thinner liquid cryogen layer and enhanced convective contribution to heat transport across the target-cryogen interface can contribute to the larger h observed with *wide* nozzles, as noted in Fig. 6(c). Fig. 7 shows a schematic of the above-described difference in spray depositions for both types of sprays: Fig. 7(a)–(c) for the finely atomized sprays produced by *narrow* nozzles and Fig. 7(d)–(f) for coarse sprays produced by *wide* nozzles.

The spray temperature measurements shown in Fig. 4 may not reflect the cryogen layer average temperature (T_c) when a solid object is placed at the same nozzle-to-surface distance.
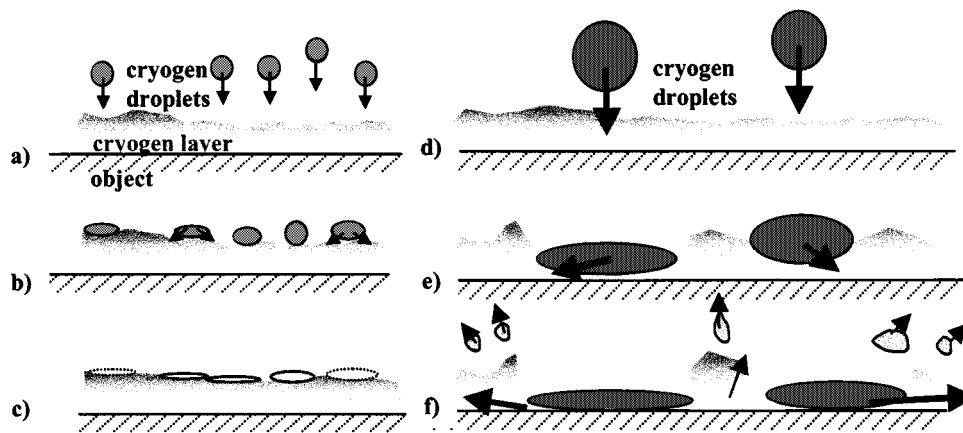
Fig. 7. Sketches (a) though (c) illustrate three different stages of how relatively small droplets produced by *narrow nozzles* may impinge on the sprayed object and form a cryogen layer, which incoming droplets may not easily penetrate. In contrast, in sketches (d) through (f), larger droplets produced by the *wide nozzles* may splash off and pierce through cryogen deposited on the surface, giving place to a thinner layer and, also reaching a better thermal contact with the sprayed object.

The reason for this is that high velocity cryogen droplets and vapor that flow around the thermocouple bead may actually enhance the convection and evaporation of liquid cryogen in contact with the thermocouple bead and, thus, result in lower temperatures. This effect may be even more pronounced for fine sprays, where the gas (air and cryogen vapor)-to-liquid ratio at any point within the spray is presumably larger. However, the obvious alternative of placing a thermocouple sensor on top of the sprayed surface has known drawbacks. In that case, the thermocouple may measure the average temperature of the cryogen layer, in which a large temperature gradient may exist. Furthermore, if the cryogen layer is smaller than the dimension of the thermocouple bead, the measured temperature reflects an average of the gas on top of the cryogen layer and the layer itself. Such an effect is very likely, since the smallest commercially available thermocouple beads are 30 μm in diameter, while the cryogen layers are estimated at $\approx$ 20 μm thick [21]. Using the copper rod method and above-presented analysis, however, it is not necessary to measure T_c independently. From the presented data, we obtained estimates of $T_c \approx -43\,°C$ and $-44\,°C$ for nozzles SN and SW, respectively. These values are 4 °C to 8 °C higher than those measured with a thermocouple positioned in the spray axis at the same distance from the nozzle for the *narrow* ($T = -55\,°C$) and *wide* ($T = -48\,°C$) nozzles [10], in agreement with the explanation presented above.

Our previous work [14] showed that the time evolution of temperature measured by thermocouples embedded in an epoxy block and positioned 3 mm from the spray axis, was significantly different than in the center of the spray. However, our measurements indicated that the lateral variation of spray temperature (Fig. 4) is negligible over a cross section of 12 mm in diameter, but varies considerably toward the periphery. This suggests that other relevant spray characteristics (e.g., droplet diameter, velocity) are inconsistent over the entire sprayed area. The cause for such lateral inhomogeneity is that droplets closer to the edge of the spray are subjected to larger drag forces while moving through steady air and are in closer contact with the warmer environment (air), thus heating up faster. It is expected that these differences should appear in future spatially resolved measurements as lateral variations of q_s and, thus, of h.

One advantage of the steady-state method is that it enables us to study the heat transfer mechanisms of CSC when spraying objects of a constant surface temperature. In earlier studies, h was found to be significantly different for surface temperatures above and below the medium cryogen boiling temperature [23]. Unfortunately, due to the lack of experimental data around the cryogen boiling temperature ($-26\,°C$), our results do not conclusively confirm, nor exclude the presence of such an effect for the SN nozzle, but do exclude it for the SW. Quantitatively, we believe that the determined values of h (15 000–35 000 W/m^2·K for the SN; 32 000–42 000 W/m^2 · K for the SW nozzle) are very realistic. Typical values for forced convection in the literature are reportedly in the range of 50–20 000 W/m^2 · K and 2500–100 000 W/m^{2}K for convection involving a phase transition [24].

A drawback of the presented method is that it may not be suitable for evaluation of short spurts, as used in current clinical applications (20–100 ms), due to the fact that transient phenomena is likely to be dominant in this case. Therefore, it is important to note that the values reported above are not to be compared directly with h estimates from experiments involving such short spurts. Due primarily to the relatively long spray development time [10], heat extraction during the first 20–30 ms of spraying can be expected to be significantly smaller than the steady-state value [17]. As an example, using the epoxy-block technique, we have obtained an average estimate of $h =$ 10 000 $(+20\,000/-4000)$ W/m^2·K during a 150-ms spurt from the LW nozzle [14]. More recently, we have introduced a similar experimental technique, which permits determination of q_s and h, during short cryogen spurts. Systematic measurements resulted in an average h value around 6400 W/m^2 · K for 50 ms or longer spurts from the ScleroPlus commercial cryogen spray device ($d_N \approx 0.75$ mm, $l_N \approx 25$ mm) [18]. This result is in agreement with more recent measurements taken with a similar nozzle (SN), where a time-dependent $h(t)$ reached a peak value of ~ 8000 W/m^2 · K (somewhat depending on the T_c estimate) after an 80-ms spurt [17].

Note, however, that even if h can be estimated very accurately with either of these methods, it may not be directly applicable to spraying human skin. The surface of human skin is not as

smooth as that of an epoxy block or metal rod, has different chemical composition and likely exhibits a temporal variation of surface temperature during short spurts. Moreover, it has been suggested that CSC of human skin involves a significant storage of latent heat due to transient freezing of water [25].

In terms of spatial cooling selectivity—the premise of CSC in laser dermatologic surgery, coarser sprays (*wide nozzles*) seem preferable. However, with the nozzles investigated in this study, these sprays are poorly localized on the cooled area. Moreover, their higher-momentum impact on skin is considerably more uncomfortable for the patient as opposed to the more gentle deposition of finer sprays. If, in future nozzle designs, the magnitude of h can be sustained at sufficiently large values (10 000 W/m$^2 \cdot$ K or higher), while keeping the spray impact comfortable, such a design would be preferable over current commercial nozzles and even the *wide* and *narrow nozzle* geometries investigated herein. If this is not possible, a compromise between spray localization and patient comfort must be achieved for improved cooling selectivity and enhance of acceptance and therapeutic outcome during PWS laser therapy.

One way to increase droplet momentum while keeping a cone-type spray would be to study the role of nozzle length (l_N) in more detail. The differences in average droplet velocities we have seen between the *narrow* and *wide nozzles* may be more significant than those seen for average droplet diameters. The possibility still exists to reduce l_N below 32 mm and, hopefully, obtain the advantages of larger h and larger covered area with patient comfort. Two alternative approaches, not yet fully explored, might be to optimize cooling performance by carefully adjusting the spraying distance for a specific nozzle and application [18], or employ sequential (i.e., intermittent) spurts, where mass flux can be correlated with evaporation rate on the skin surface without adversely affecting the main spray characteristics [17].

V. CONCLUSION

FFLP images show that *narrow* nozzles ($d_N = 0.7$ mm) produce cone-shaped finely atomized sprays, which are deposited gently on the impact zone of the sprayed surface. A layer of liquid cryogen builds up when the delivered mass flux exceeds the evaporation rate. In contrast, *wide* nozzles ($d_N = 1.4$) produce jet-like coarser sprays, capable of pushing excess cryogen away from the impact area, thus causing it to dry quicker after spurt termination.

We have developed a novel experimental approach which enables reproducible and accurate determination of q_s and h during continuous CSC. The method utilizes measurements of steady-state temperature profiles in a thin copper rod at an adjustable target surface temperature (T_s), which provides new insight into the mechanisms of heat transfer across the target-cryogen interface during CSC.

In the explored range of T_s (from $-32\,^\circ$C to $-7\,^\circ$C), q_s using the *narrow* nozzle increased monotonically from ~ 15 to 130 W/cm^2 and is approximately twice as high with the *wide* nozzle. The corresponding values of h increase nonlinearly from 15 000

to 35 000 W/m$^2 \cdot$ K for the *narrow* nozzle, whereas they are significantly higher and almost independent of T_s (32 000–40 000 W/m$^2 \cdot$ K) with the *wide* nozzle.

The presented results conclusively support a formerly presented hypothesis that the liquid cryogen layer, as deposited by the *narrow* atomizing nozzles, can significantly impair the rate of heat extraction from cooled human skin. In contrast, larger-momentum droplets from coarse sprays (*wide* nozzles) pierce through the cryogen layer and displace the (warmer) liquid cryogen layer toward the periphery. Consequently, both the reduced thickness of the liquid layer and enhanced convection therein contribute to the larger q_s observed with *wide* nozzles. Unfortunately, since such coarse sprays are accompanied by poor localization of the cooled area and their impact on human skin is uncomfortable, further approaches to optimization of CSC devices for dermatologic laser surgery must be investigated.

REFERENCES

[1] C. J. Chang and J. S. Nelson, "Cryogen spray cooling and higher fluence pulsed dye laser treatment improve port-wine stain clearance while minimizing epidermal damage," *Dermatol. Surg.*, vol. 25, pp. 767–772, 1999.

[2] A. J. Welch, M. Motamedi, and A. Gonzalez, "Evaluation of cooling techniques for the protection of the epidermis during Nd:YAG laser irradiation of the skin," in *Nd-YAG Laser in Medicine and Surgery*. New York: Elsevier, 1983.

[3] J. S. Nelson, T. E. Milner, B. Anvari, B. S. Tanenbaum, S. Kimel, L. O. Svaasand, and S. L. Jacques, "Dynamic epidermal cooling during pulsed laser treatment of port-wine stain: A new methodology with preliminary clinical evaluation," *Arch. Dermatol.*, vol. 131, pp. 695–700, 1995.

[4] B. Anvari, B. S. Tanenbaum, T. E. Milner, S. Kimel, L. O. Svaasand, and J. S. Nelson, "A theoretical study of the thermal response of skin to cryogen spray cooling and pulsed laser irradiation—implications for treatment of port wine stain birthmarks," *Phys. Med. Biol.*, vol. 40, pp. 1451–1465, 1995.

[5] H. A. Waldorf, T. S. Alster, K. McMillan, A. N. Kauvar, R. G. Geronemus, and J. S. Nelson, "Effect of dynamic cooling on 585-nm pulsed dye laser treatment of port-wine stain birthmarks," *Dermatol. Surg.*, vol. 23, pp. 657–662, 1997.

[6] C. J. Chang, B. Anvari, and J. S. Nelson, "Cryogen spray cooling for spatially selective photocoagulation of hemangiomas: a new methodology with preliminary clinical reports," *Plast. Reconstr. Surg.*, vol. 102, pp. 459–463, 1998.

[7] K. M. Kelly, J. S. Nelson, G. P. Lask, R. G. Geronemus, and L. J. Bernstein, "Cryogen spray cooling in combination with nonablative laser treatment of facial rhytides," *Arch. Dermatol.*, vol. 135, pp. 691–694, 1999.

[8] G. B. Altshuler, H. H. Zenzie, A. V. Erofeev, M. Z. Smirnov, R. R. Anderson, and C. Dierickx, "Contact cooling of the skin," *Phys. Med. Biol.*, vol. 44, pp. 1003–1023, 1999.

[9] J. S. Nelson, B. Majaron, and K. M. Kelly, "Active skin cooling in conjunction with laser dermatologic surgery," *Semin. Cutan. Med. Surg.*, vol. 19, pp. 253–266, 2000.

[10] G. Aguilar, B. Majaron, W. Verkruysse, J. S. Nelson, and E. J. Lavernia, "Characterization of cryogenic spray nozzles with application to skin cooling," in *Proc. ASME*, vol. FED-253, New York, 2000, pp. 189–197.

[11] G. Aguilar, W. Verkruysse, B. Majaron, Y. Zhou, J. S. Nelson, and E. J. Lavernia, "Modeling cryogenic spray temperature and evaporation rate based on single-droplet analysis," in *Proc. 8th Int. Conf. Liq. Atom. Spray Syst.*, Pasadena, CA, July 16–20, 2000, pp. 1041–1046.

[12] G. Aguilar, B. Majaron, W. Verkruysse, Y. Zhou, J. S. Nelson, and E. J. Lavernia, "Theoretical and experimental analysis of droplet diameter, temperature and evaporation rate evolution in cryogenic sprays," *Int. J. Heat Mass Transfer*, vol. 44, pp. 3201–3211, 2001.

[13] J. H. Torres, J. S. Nelson, B. S. Tanenbaum, T. E. Milner, D. M. Goodman, and B. Anvari, "Estimation of internal skin temperature measurements in response to cryogen spray cooling: implications for laser therapy of port wine stains," *IEEE J. Select. Topics Quantum Electron.*, vol. 5, pp. 1058–1066, July/Aug. 1999.

[14] W. Verkruysse, B. Majaron, G. Aguilar, L. O. Svaasand, and J. S. Nelson, "Dynamics of cryogen deposition relative to heat extraction rate during cryogen spray cooling," *Proc. SPIE*, vol. 3907, 2000.

[15] W. Verkruysse, B. Majaron, B. S. Tanenbaum, and J. S. Nelson, "Optimal cryogen spray cooling parameters for pulsed laser treatment of port wine stains," *Lasers Surg. Med.*, vol. 27, pp. 165–170, 2000.

[16] J. W. Valvano and J. Pearce, "Temperature measurements," in *Optical Thermal Response of Laser Irradiated Tissue*, A. J. Welch and M. J. C. van Gemert, Eds. New York: Plenum, 1995, p. 515.

[17] B. Majaron, G. Aguilar, B. Basinger, L. L. Randeberg, L. O. Svaasand, E. J. Lavernia, and J. S. Nelson, "Sequential cryogen spraying for heat flux control at the skin surface," *Proc. SPIE*, vol. 4244, 2001.

[18] G. Aguilar, B. Majaron, K. Pope, L. O. Svaasand, J. S. Nelson, and E. J. Lavernia, "Influence of nozzle-to-skin distance in cryogen spray cooling for dermatologic laser surgery," *Lasers Surg. Med.*, vol. 28, pp. 113–120, 2001.

[19] B. Majaron, S. Kimel, W. Verkruysse, G. Aguilar, K. Pope, L. O. Svaasand, E. J. Lavernia, and J. S. Nelson, "Cryogen spray cooling in laser dermatology: effects of ambient humidity and frost formation," *Lasers Surg. Med.*, vol. 28, 2001.

[20] H. S. Carslaw and J. C. Jaeger, *Conduction of Heat in Solids*, 2nd ed. Oxford, U.K.: Oxford Science, 1959, p. 20.

[21] B. Anvari, T. E. Milner, B. S. Tanenbaum, S. Kimel, L. O. Svaasand, and J. S. Nelson, "Dynamic epidermal cooling in conjunction with laser treatment of port wine stains: theoretical and preliminary clinical evaluations," *Lasers Med. Sci.*, vol. 10, pp. 105–112, 1996.

[22] B. M. Pikkula, J. H. Torres, J. W. Tunnell, and B. Anvari, "Cryogen spray cooling: effects of droplet size and spray density on heat removal," *Lasers Surg. Med.*, vol. 28, pp. 103–112, 2001.

[23] K. A. Estes and I. Mudawar, "Correlation of sauter mean diameter and critical heat flux for spray cooling of small surfaces," *Int. J. Heat Mass Transfer*, vol. 38, pp. 2985–2996, 1995.

[24] F. P. Incropera and D. P. DeWitt, *Fundamentals of Heat and Mass Transfer*, 4th ed. New York: Wiley, 1996.

[25] H. H. Zenzie, G. B. Altshuler, M. Z. Smirnov, and R. R. Anderson, "Evaluation of cooling methods for laser dermatology," *Lasers Med. Surg.*, vol. 26, pp. 130–144, 2000.

Guillermo Aguilar received the B.S. degree in mechanical engineering from the National Autonomous University of Mexico in 1993 and the M.S. and Ph.D. degrees in mechanical engineering from the University of California at Santa Barbara in 1995 and 1999, respectively.

He was a Postdoctoral Researcher with the Beckman Laser Institute and the Department of Chemical end Biochemical Engineering and Material Science, University of California, Irvine (UCI), where he is currently an Assistant Professor at the Center for Biomedical Engineering. His research interests include cryogen spray atomization and heat transfer, application of cryogen sprays and laser irradiation in dermatology, and therapeutic applications of lasers in dermatology and reconstructive surgery.

Wim Verkruysse received his B.S. and Ph.D. degrees in physics in 1986 and 1993, respectively, from the University of Amsterdam, Amsterdam, The Netherlands.

He was a Postdoctoral Researcher with the Beckman Laser Institute and Medical Clinic, University of California, Irvine, from 1998 to 2000.

Boris Majaron received the B.S., M.S., and Ph.D. degrees in physics from the University of Ljubljana, Slovenia, in 1985, 1989, and 1993, respectively.

Since 1993, he has been with Joef Stefan Institute, Ljubljana. His research experience includes laser spectroscopy of strongly doped laser materials, nonlinear optics, and laser technology. His research in the field of biomedical optics involves therapeutic laser applications for dermatology and dentistry, cryogen spray cooling, and pulsed photothermal radiometry.

Lars O. Svaasand was born in Oslo, Norway, in 1938. He received the M.Sc. degree in electrical engineering in 1961 and the Ph.D. degree in physical electronics in 1974, both from the Norwegian Institute of Technology.

He is currently Professor of physical electronics at the Norwegian University of Science and Technology, and has been a Visiting Scientist at Beckman Laser Institute and Medical Clinic, University of California, Irvine, since 1999. He has been engaged in research on medical applications of lasers since 1980.

Enrique J. Lavernia received the B.S. degree in solid mechanics from Brown University, Providence, RI, in 1982, the M.S. degree in metallurgy from the Massachusetts Institute of Technology (MIT), Cambridge, in 1984, and the Ph.D. degree in materials engineering from MIT in 1986.

Since 1998, he has been Professor and Chair of the Department Chemical Engineering and Material Science, University of California, Irvine (UCI). He also holds joint appointments with the Department of Mechanical and Aerospace Engineering and the Center for Biomedical Engineering. His research interests are the processing of structural materials and metal matrix composites with particular emphasis on solidification fundamentals, rapid solidification processing, spray atomization and deposition of structural materials, solidification processing of metal matrix composites, and mathematical modeling of advanced materials and processes.

J. Stuart Nelson receive the M.D. degree from the University of Southern California, Los Angeles, and the Ph.D. degree from the University of California (UC), Irvine.

He is the Associate Director at the Beckman Laser Institute and Medical Clinic and a full-time Professor in the Departments of Surgery, Dermatology, and Biomedical Engineering, UC, Irvine. His research interests include studies at both the basic science and applied levels. The basic science studies fall into two specific areas: 1) the biophysics of laser interaction with biological tissues and 2) the understanding of structural changes produced in tissues by laser light. At the applied level, his research objectives are in developing new approaches to the diagnosis and treatment of diseases amenable to laser therapy.